

## On the Reactivity of Surface Methoxy Species in Acidic Zeolites

Yijiao Jiang, Michael Hunger, and Wei Wang\*

Contribution from the Institute of Chemical Technology, University of Stuttgart,  
D-70550 Stuttgart, Germany

Received February 22, 2006; E-mail: weiwang\_lanzhou@yahoo.com

**Abstract:** The in situ preparation and isolation of surface methoxy species on acidic zeolites are followed by further investigations of their reactivity in heterogeneously catalyzed reactions. For the first time, the following solid-state NMR evidence for the high reactivity of surface methoxy species has been obtained: (i) Surface methoxy species react readily with ammonia on acidic zeolites at room temperature, by which methylamines and methylammonium cations are formed. (ii) The transformation of surface methoxy species to other alkoxy species can be achieved by the reaction of surface methoxy species and corresponding alkyl halides on acidic zeolites. (iii) Surface methoxy species react readily with hydrochloride, giving methyl chloride as the sole product. (iv) The classic Koch carbonylation reaction and Ritter reaction in solution can be performed with surface methoxy species on acidic zeolites. (v) Carbon monoxide and carbon dioxide are produced by the oxidation of surface methoxy species in the presence of oxygen. The stability and reactivity of surface methoxy species are discussed in comparison with other surface alkoxy species ( $>C_1$  species).

### Introduction

Knowledge of the mechanisms involved in heterogeneously catalyzed reactions is of fundamental interest and may also be of value for the optimization of existing industrial processes and for the development of new ones. Carbenium ions were considered as likely intermediates<sup>1,2</sup> involved in a variety of reactions catalyzed by acidic zeolites. However, the efforts to experimentally verify the long-lived existence of simple alkyl cations, e.g., isopropyl or *tert*-butyl cations, in acidic zeolites have been in vain so far.<sup>3–6</sup> It was suggested by Kazansky<sup>7</sup> that free carbenium cations mostly exist as transition states rather than as persistent intermediates in acid-catalyzed reactions performed on acidic zeolites. Instead, the surface alkoxy (alkoxide) species with carbenium-ion-like properties<sup>4</sup> may act as catalytic intermediates in zeolite chemistry.<sup>7</sup> This topic has been stimulating extensive research interest, and important progress has recently been made by using theoretical calculations.<sup>8–13</sup> Due to the complexity of the heterogeneous system under study,

however, experimental evidence for the existence and reactivity of surface alkoxy species<sup>3–6,14–16</sup> is still lacking or ambiguous.

By an in situ stopped-flow MAS NMR technique, we have been able to observe the formation of surface methoxy species

- (1) Jacobs, P. A. *Carboniogenic Activity of Zeolites*; Elsevier: New York, 1977.
- (2) Olah, G. A.; Prakash, G. K. S.; Sommer, J. *Superacids*; Wiley-Interscience: New York, 1985.
- (3) (a) Noguchi, H.; Yoda, E.; Ishizawa, N.; Kondo, J. N.; Wada, A.; Kobayashi, H.; Domen, K. *J. Phys. Chem. B* **2005**, *109*, 17217–17223 and references therein. (b) Kondo, J. N.; Ito, K.; Yoda, E.; Wakabayashi, F.; Domen, K. *J. Phys. Chem. B* **2005**, *109*, 10969–10972.
- (4) (a) Aronson, M. T.; Gorte, R. J.; Farneth, W. E.; White, D. *J. Am. Chem. Soc.* **1989**, *111*, 840–846. (b) Farneth, W. E.; Gorte, R. *J. Chem. Rev.* **1995**, *95*, 615–635.
- (5) Stepanov, A. G.; Romannikov, V. N.; Zamaraev, K. I. *Catal. Lett.* **1992**, *13*, 395–405.
- (6) (a) Haw, J. F.; Richardson, B. R.; Oshiro, I. S.; Lazo, N. D.; Speed, J. A. *J. Am. Chem. Soc.* **1989**, *111*, 2052–2058. (b) Haw, J. F.; Nicholas, J. B.; Xu, T.; Beck, L. W.; Ferguson, D. B. *Acc. Chem. Res.* **1996**, *29*, 259–267.
- (7) (a) Kazansky, V. B. *Catal. Today* **1999**, *51*, 419–434. (b) Kazansky, V. B. *Acc. Chem. Res.* **1991**, *24*, 379–383.

- (8) (a) Tuma, C.; Sauer, J. *Angew. Chem., Int. Ed.* **2005**, *44*, 4769–4771. (b) Nieminen, V.; Sierka, M.; Murzin, D. Y.; Sauer, J. *J. Catal.* **2005**, *231*, 393–404. (c) Clark, L. A.; Sierka, M.; Sauer, J. *J. Am. Chem. Soc.* **2004**, *126*, 936–947. (d) Clark, L. A.; Sierka, M.; Sauer, J. *J. Am. Chem. Soc.* **2003**, *125*, 2136–2141.
- (9) (a) Boronat, M.; Viruela, P. M.; Corma, A. *J. Am. Chem. Soc.* **2004**, *126*, 3300–3309. (b) Boronat, M.; Zicovich-Wilson, C. M.; Viruela, P.; Corma, A. *J. Phys. Chem. B* **2001**, *105*, 11169–11177. (c) Boronat, M.; Viruela, P.; Corma, A. *Phys. Chem. Chem. Phys.* **2001**, *3*, 3235–3239. (d) Boronat, M.; Zicovich-Wilson, C. M.; Viruela, P.; Corma, A. *Chem.—Eur. J.* **2001**, *7*, 1295–1303.
- (10) (a) Rozanska, X.; Barbosa, L. A. M. M.; van Santen, R. A. *J. Phys. Chem. B* **2005**, *109*, 2203–2211. (b) Rozanska, X.; van Santen, R. A.; Demuth, T.; Hutschka, F.; Hafner, J. *J. Phys. Chem. B* **2003**, *107*, 1309–1315. (c) Demuth, T.; Rozanska, X.; Benco, L.; Hafner, J.; van Santen, R. A.; Toulhoat, H. *J. Catal.* **2003**, *214*, 68–77. (d) Rozanska, X.; Demuth, T.; Hutschka, F.; Hafner, J.; van Santen, R. A. *J. Phys. Chem. B* **2002**, *106*, 3248–3254. The reactivity theory of Brønsted Acid Sites was discussed in: (e) van Santen, R. A. *Chem. Rev.* **1995**, *95*, 637–660.
- (11) (a) Vos, A. M.; Schoonheydt, R. A.; De Proft, F.; Geerlings, P. *J. Phys. Chem. B* **2003**, *107*, 2001–2008. (b) Vos, A. M.; Nulens, K. H. L.; De Proft, F.; Schoonheydt, R. A.; Geerlings, P. *J. Phys. Chem. B* **2002**, *106*, 2026–2034.
- (12) (a) Svelle, S.; Kolboe, S.; Swang, O.; Olsbye, U. *J. Phys. Chem. B* **2005**, *109*, 12874–12878. (b) Svelle, S.; Kolboe, S.; Swang, O. *J. Phys. Chem. B* **2004**, *108*, 2953–2962. (c) Svelle, S.; Arstad, B.; Kolboe, S.; Swang, O. *J. Phys. Chem. B* **2003**, *107*, 9281–9289. (d) Svelle, S.; Kolboe, S.; Olsbye, U.; Swang, O. *J. Phys. Chem. B* **2003**, *107*, 5251–5260.
- (13) (a) Joshi, Y. V.; Bhan, A.; Thomson, K. T. *J. Phys. Chem. B* **2004**, *108*, 971–980. (b) Bhan, A.; Joshi, Y. V.; Delgass, W. N.; Thomson, K. T. *J. Phys. Chem. B* **2003**, *107*, 10476–10487.
- (14) Wang, W.; Jiao, J.; Jiang, Y.; Ray, S. S.; Hunger, M. *ChemPhysChem* **2005**, *6*, 1467–1469 and references therein.
- (15) (a) Bosacek, V.; Klik, R.; Genoni, F.; Spano, G.; Rivetti, F.; Figueras, F. *Magn. Reson. Chem.* **1999**, *37*, S135–S141. (b) Bosacek, V.; Ernst, H.; Freude, D.; Mildner, T. *Zeolites* **1997**, *18*, 196–199. (c) Bosacek, V. *J. Phys. Chem.* **1993**, *97*, 10732–10737.
- (16) (a) Forester, T. R.; Howe, R. F. *J. Am. Chem. Soc.* **1987**, *109*, 5076–5082. (b) Forester, T. R.; Wong, S. T.; Howe, R. F. *J. Chem. Soc., Chem. Commun.* **1986**, 1611–1613.

from methanol<sup>17</sup> and surface ethoxy species from ethanol<sup>14</sup> on acidic zeolites. Furthermore, the intermediary role of surface methoxy species in the methanol-to-olefin (MTO) process was demonstrated.<sup>17</sup> On acidic zeolites at reaction temperatures lower than 473 K, surface methoxy species act as reactive methylating agents, which can react with methanol to form dimethyl ether (DME)<sup>17a</sup> and with toluene to form xylenes.<sup>17c</sup> At reaction temperatures higher than 523 K, the decomposition of surface methoxy species takes place as a result of dissociation of the C–H bond of the methyl group, which is further responsible for the first C–C coupling and, therefore, for the formation of primary hydrocarbons in the MTO process.<sup>17c,d</sup>

The approach we developed<sup>17</sup> for the in situ preparation of surface methoxy species allows us to further investigate the reactivity of surface methoxy species in heterogeneously catalyzed reactions. In this contribution, <sup>13</sup>C MAS NMR spectroscopy is utilized to study the reactions of surface methoxy species with ammonia, alkyl halides, hydrochloride, carbon monoxide, acetonitrile, and oxygen on solid acid catalysts. On the basis of these experimental findings, the reactivity of surface methoxy species is discussed in terms of C–O bond and C–H bond activation, respectively. By benefit of recent theoretical investigations, the relative stability and reactivity of surface alkoxy species in acidic zeolites are further compared.

## Experimental Section

**Materials.** Zeolite Na–Y ( $n_{\text{Si}}/n_{\text{Al}} = 2.7$ ) was purchased from Degussa AG, Hanau, Germany. The NH<sub>4</sub>–Y zeolite was prepared by a four-fold ion exchange of zeolite Na–Y at 353 K in a 1.0 M aqueous solution of NH<sub>4</sub>NO<sub>3</sub>. After an ion-exchange degree of 90% was reached, the material was washed in demineralized water and dried at room temperature. Subsequently, the NH<sub>4</sub>–Y zeolite was heated in a vacuum with a rate of 20 K/h up to the final temperature of 723 K. There, the material was calcined at a pressure below 10<sup>–2</sup> mbar for 12 h leading to zeolite H–Y. The silicoaluminophosphate H–SAPO-34 with an  $n_{\text{Si}}/(n_{\text{Al}} + n_{\text{Si}} + n_{\text{P}})$  ratio of 0.11 was prepared according to the recipe described in ref 18 for the synthesis of Ni–SAPO-34, but omitting the nickel salt. To remove the template, the as-synthesized material was heated at a rate of 60 K/h to 873 K in dry nitrogen and calcined at this temperature for 6 h in synthetic air (20 vol % oxygen, 60 L/h). Subsequently, the sample was subjected to additional calcination in a vacuum with a heating rate of 20 K/h up to the final temperature of 673 K. At this temperature, the material was calcined at a pressure below 10<sup>–2</sup> mbar for 12 h leading to silicoaluminophosphate H–SAPO-34. The dehydrated catalysts were sealed in glass tubes until their further use. All catalysts were characterized by AES-ICP, XRD, and solid-state <sup>1</sup>H, <sup>27</sup>Al, and <sup>29</sup>Si MAS NMR spectroscopy. The results indicated that the material obtained after cation exchange and calcination was neither damaged nor dealuminated. <sup>13</sup>C-Enriched methanol (<sup>13</sup>C-enrichment of 99%), <sup>13</sup>C-enriched methyl iodide (<sup>13</sup>C-enrichment of 99%), and <sup>13</sup>C-1-enriched ethyl iodide (<sup>13</sup>C-1-enrichment of 99%) were purchased from Cambridge Isotopes. <sup>13</sup>C-Enriched carbon monoxide (<sup>13</sup>C-enrichment of 99%) was purchased from Aldrich.

**Sample Preparation.** The in situ preparation of surface methoxy species from <sup>13</sup>C-enriched methanol on acidic catalysts H–Y and H–SAPO-34 was described elsewhere.<sup>17</sup> By <sup>13</sup>C spinning-counting experiments, the coverage of surface methoxy species was determined

as ca. 0.44 per acid site on acidic zeolite H–Y, which agrees well with our previous results.<sup>17d</sup> The methylated catalyst (ca. 300 mg) was then loaded with a volatile reactant on a vacuum line and fused in a glass tube (outer diameter of ca. 6 mm and length of ca. 180 mm) for further thermal treatment. After heating, the glass tube was opened in a glovebox, and the catalyst was transferred into a 7 mm MAS NMR rotor for solid-state MAS NMR measurements. In the case of oxidation reaction, the methylated catalyst was transferred into an MAS NMR insert (Wilmad, 5.6 mm o.d. with constrictions) inside a glovebox and loaded with ca. 5 mbar of oxygen and, subsequently, sealed. The sealed glass inserts were heated to the reaction temperature for 20 min.

**<sup>13</sup>C MAS NMR Experiments.** All <sup>13</sup>C MAS NMR investigations were performed with a 7 mm Bruker MAS NMR probe on a Bruker MSL-400 spectrometer at a <sup>13</sup>C resonance frequency of 100.6 MHz. <sup>13</sup>C high-power proton decoupling (HPDEC) MAS NMR spectra were recorded after an excitation with a  $\pi/2$  pulse and with a repetition time of 5 s. For <sup>13</sup>C spin-counting experiments, a repetition time of 30 s was performed, and an external intensity standard (dehydrated zeolite H–Y loaded with <sup>13</sup>CH<sub>3</sub>OH) was applied. <sup>13</sup>C cross-polarization (CP) MAS NMR spectra were performed with a contact time of 5 ms and with a repetition time of 2 s. The sample spinning rates of ca. 3.5 to 4.5 kHz were applied. All <sup>13</sup>C MAS NMR spectra were referenced to tetramethylsilane (TMS).

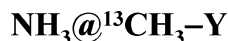
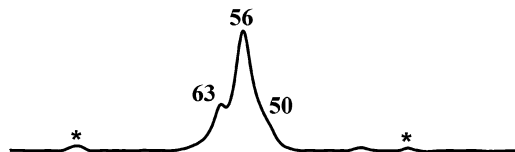
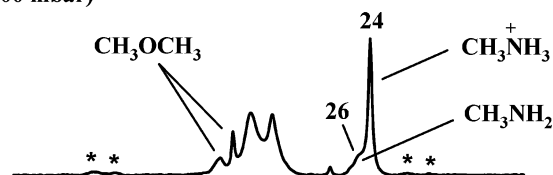
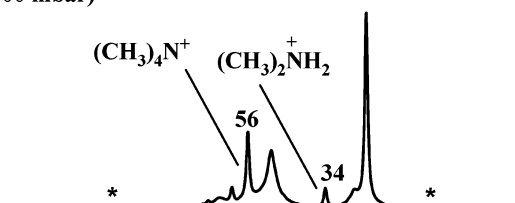
## Results

**Reaction of Surface Methoxy Species and Ammonia at Room Temperature.** Heterogeneously catalyzed alkylation of amines by alcohols, for example, the methylation of ammonia by methanol on zeolite catalysts,<sup>19–22</sup> has attracted significant interest in recent years. Different mechanisms have been proposed for the reaction of methanol and ammonia on acidic zeolites.<sup>20</sup> It has been suggested that ammonia and methylamines are preferentially adsorbed on Brønsted acid sites, due to their higher proton affinities in the gas phase than that of methanol.<sup>20</sup> Therefore, most of the proposed mechanisms assume that the reaction does not involve surface methoxy species.<sup>20</sup> However, the existence of surface methoxy species has been experimentally observed by in situ IR spectroscopy during the reaction of methanol and ammonia on acidic zeolite H–ZSM-5.<sup>22</sup> In addition, the formation of surface methoxy species during aniline methylation on acidic zeolite H–Y has been shown with the application of in situ MAS NMR spectroscopy.<sup>23,24</sup> In this contribution, the reaction of surface methoxy species and ammonia was, therefore, studied by <sup>13</sup>C MAS NMR spectroscopy. It was found that surface methoxy species react readily with ammonia on acidic zeolite H–Y and silicoaluminophosphate H–SAPO-34 at room temperature, by which methylamines and methylammonium cations are formed.

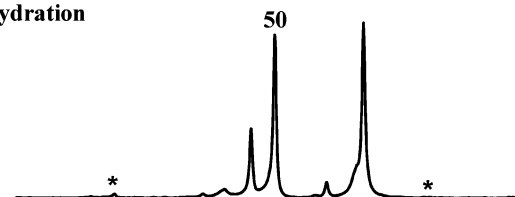
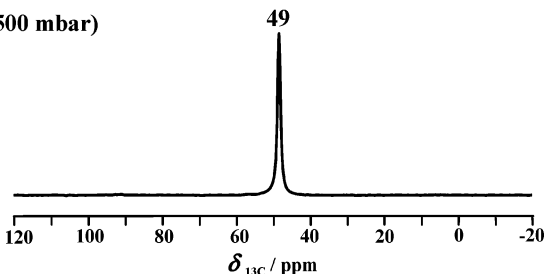
For convenience of comparison, Figure 1a shows again the <sup>13</sup>C MAS NMR spectrum recorded after the in situ preparation of surface methoxy species (<sup>13</sup>CH<sub>3</sub>–Y) on zeolite H–Y from the <sup>13</sup>C-enriched methanol.<sup>17</sup> The dominating signal at 56 ppm with spinning sidebands is due to surface methoxy species.<sup>17</sup>

- (17) (a) Wang, W.; Seiler, M.; Hunger, M. *J. Phys. Chem. B* **2001**, *105*, 12553–12558. (b) Wang, W.; Buchholz, A.; Arnold, A.; Xu, M.; Hunger, M. *Chem. Phys. Lett.* **2003**, *370*, 88–93. (c) Wang, W.; Buchholz, A.; Seiler, M.; Hunger, M. *J. Am. Chem. Soc.* **2003**, *125*, 15260–15267. (d) Jiang, Y.; Wang, W.; Marthala, V. R. R.; Huang, J.; Sulikowski, B.; Hunger, M. *J. Catal.* **2006**, *238*, 21–27.
- (18) Kang, M.; Inui, T. *J. Mol. Catal. A: Chem.* **1999**, *140*, 55–63.

- (19) Veefkind, V. A.; Lercher, J. A. *Appl. Catal., A* **1999**, *181*, 245–255 and references therein.
- (20) Corbin, D. R.; Schwarz, S.; Sonnichsen G. C. *Catal. Today* **1997**, *37*, 71–102 and references therein.
- (21) Gruedling, C.; Eder-Mirth G.; Lercher J. A. *J. Catal.* **1996**, *160*, 299–308.
- (22) Chen, D. T.; Zhang, L.; Yi, C.; Dumesic, J. A. *J. Catal.* **1994**, *146*, 257–267.
- (23) Ivanova, I. I.; Pomakhina, E. B.; Rebrov, A. I.; Hunger, M.; Kolyagin, Y. G.; Weitkamp, J. *J. Catal.* **2001**, *203*, 375–381.
- (24) Wang, W.; Seiler, M.; Ivanova, I. I.; Sternberg, U.; Weitkamp, J.; Hunger, M. *J. Am. Chem. Soc.* **2002**, *124*, 7548–7554.

(a)  $^{13}\text{CH}_3\text{-Y}$ (b)  $^{13}\text{CH}_3\text{-Y} + \text{NH}_3$  (200 mbar)  
1.5  $\text{NH}_3$ (c)  $^{13}\text{CH}_3\text{-Y} + \text{NH}_3$  (500 mbar)  
3.5  $\text{NH}_3$ 

(d) sample (c), after hydration

(e)  $^{13}\text{CH}_3\text{OH} + \text{NH}_3$  (500 mbar)

**Figure 1.**  $^{13}\text{C}$  HPDEC MAS NMR spectra of methylated zeolites Y ( $^{13}\text{CH}_3\text{-Y}$ ), recorded before loading of ammonia (a), after loading of 200 mbar of ammonia at room temperature (b), after loading of 500 mbar of ammonia at room temperature (c). Spectrum d was recorded after the catalyst sample (c) was fully hydrated at room temperature. As a control experiment, spectrum e shows the  $^{13}\text{C}$  MAS NMR spectrum of acidic zeolite H-Y after loading of methanol and ammonia at room temperature, in which the  $^{13}\text{C}$  signal of methanol (49 ppm) is 1 ppm high-field shifted due to the coexistence of ammonia on the acidic zeolite H-Y. Asterisks denote spinning sidebands.

The signal at 63 ppm is originated from side-on adsorbed DME, while the broad signal at 50 ppm is caused by terminal methoxy species ( $\text{SiOCH}_3$ ).<sup>17</sup> Upon loading of 200 mbar of ammonia on the methylated zeolite Y (approximately 1.5  $\text{NH}_3$  per surface methoxy species) at room temperature, the  $^{13}\text{C}$  MAS NMR spectrum recorded is shown in Figure 1b. Accompanied by the decrease of the intensity of surface methoxy species at 56 ppm, new signals appear at 26 and 24 ppm which are assigned to methylamine,  $\text{CH}_3\text{NH}_2$ , and protonated methylamine,  $\text{CH}_3\text{NH}_3^+$ , respectively.<sup>25</sup> Upon loading of 500 mbar of ammonia on the methylated zeolite Y (approximately 3.5  $\text{NH}_3$  per surface

methoxy species) at room temperature, additional signals at 34 and 56 ppm become evident (Figure 1c). The signal at 34 ppm is due to the protonated dimethylamine,  $(\text{CH}_3)_2\text{NH}_2^+$ .<sup>24</sup> In comparison with the signal of surface methoxy species (Figure 1a), the signal at 56 ppm in Figure 1c is much narrower and, therefore, assigned to the tetramethylammonium cation,  $(\text{CH}_3)_4\text{N}^+$ , according to the literature.<sup>24–26</sup> The assignments are further supported by the  $^{13}\text{C}$  MAS NMR spectrum in Figure 1d, which was recorded after the catalyst was fully hydrated at room temperature. As indicated in Figure 1d, the signal of  $(\text{CH}_3)_4\text{N}^+$  at 56 ppm survived hydration, which<sup>17c</sup> surface methoxy species would not. As shown in Figure 1d, the broad signal at 50 ppm

(25) Thursfield, A.; Anderson, M. W.; Dwyer, J.; Hutchings, G. J.; Lee, D. J. *Chem. Soc., Faraday Trans.* **1998**, 94, 1119–1122.

(26) Ernst, H.; Pfeifer, H. J. *Catal.* **1992**, 136, 202–208.

Scheme 1

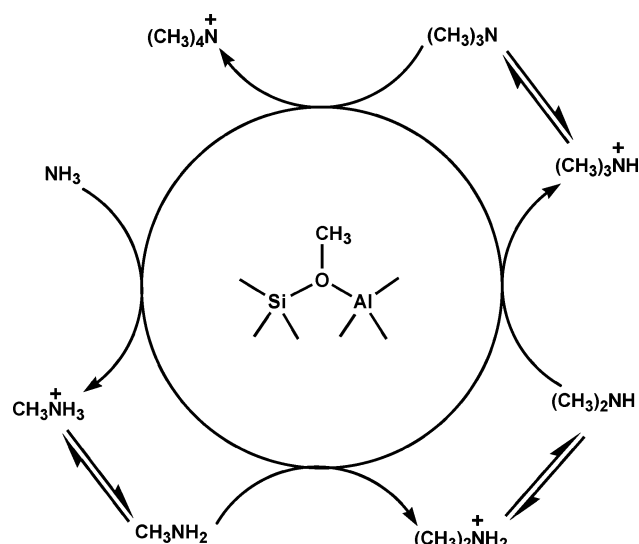


(Figure 1c) is narrowed after hydration, which indicates the reaction of terminal surface methoxy species with water to methanol.<sup>17c</sup> The reaction pathways of surface methoxy species and ammonia on zeolite Y under study are depicted in Scheme 1. Similar to the case of *N,N*-dimethylanilinium cation which has a  $^{13}\text{C}$  chemical shift of ca. 48 ppm,<sup>24</sup> the  $^{13}\text{C}$  MAS NMR signal of trimethylammonium cation,  $(\text{CH}_3)_3\text{NH}^+$ , may be overlapped by the signal at 50 ppm and, therefore, cannot be unambiguously observed in Figure 1.

It is important to note that methylamines and methylammonium cations have previously been observed<sup>25,26</sup> only after the reaction of methanol and ammonia on acidic zeolites at temperatures higher than 513 K. As shown in Figure 1b and 1c, however, the same products are readily formed via the reaction of surface methoxy species and ammonia on acidic zeolite H-Y at room temperature. As a control experiment, acidic zeolite H-Y was loaded with methanol and ammonia under identical conditions as those for preparing the sample used in Figure 1c. The  $^{13}\text{C}$  MAS NMR spectrum recorded thereafter (Figure 1e) shows only the signal of methanol at ca. 49 ppm, which indicates that methanol and ammonia do not react on acidic zeolite H-Y at room temperature. The significant difference in reactivity between surface methoxy species and methanol were also observed during the methylation of ammonia on silicoaluminophosphate H-SAPO-34 (not shown). In addition, Ivanova et al.<sup>23</sup> reported that the *N*-alkylation of aniline by surface methoxy species occurs at room temperature on zeolite H-Y. In contrast, the *N*-alkylation of aniline by methanol starts at 373 K on acidic zeolite H-Y.<sup>23,24</sup> The above-mentioned findings indicate that surface methoxy species are very reactive in methylating amines on acidic zeolites, and *if involved*, their formation is a rate-determining step during the methylation of amines by methanol on acidic zeolites. Of course, the overall reaction rate may be governed by further transfer of these methylammonium cations from the zeolite into the gas phase, which includes the methylation/demethylation (or disproportionation) and adsorption/desorption equilibria.<sup>19,20</sup>

#### Reaction of Surface Methoxy Species and Alkyl Halides.

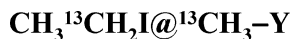
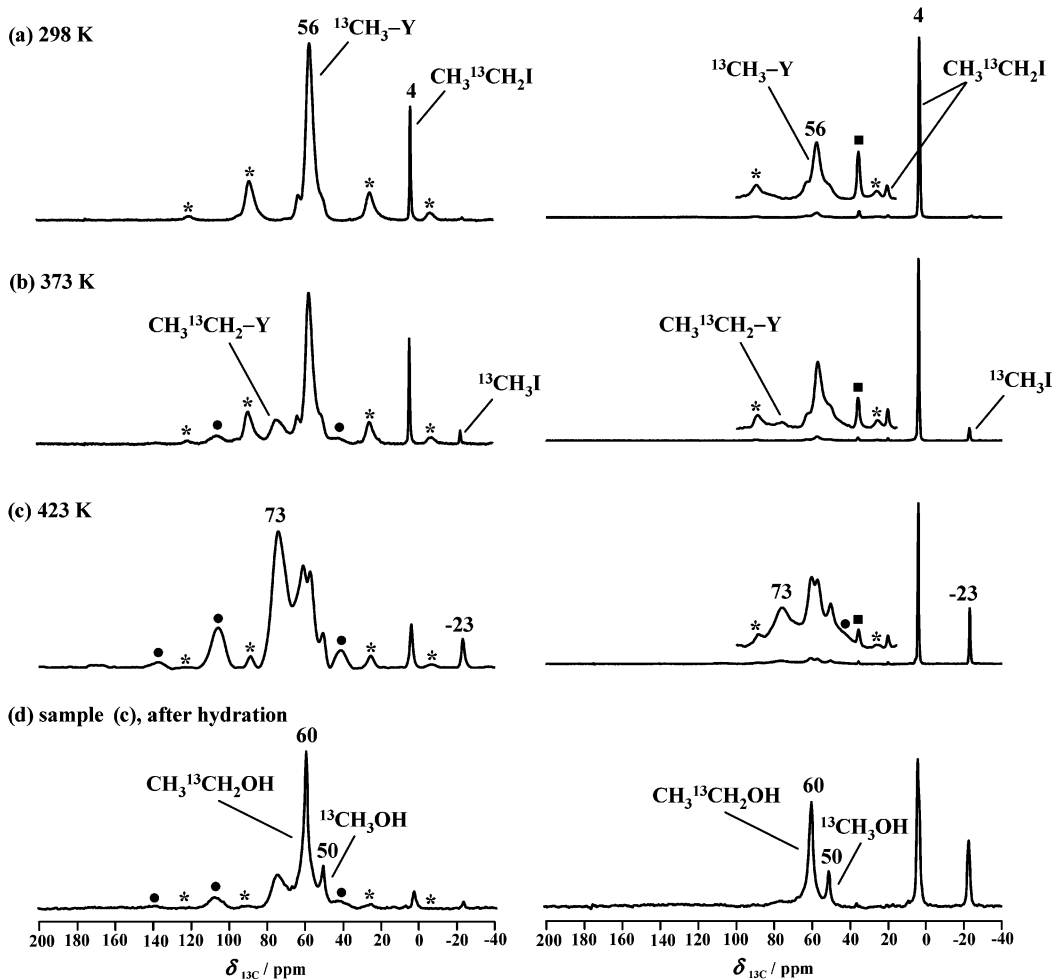
We have recently reported on the first solid-state  $^{13}\text{C}$  MAS NMR evidence for the formation of surface ethoxy species upon the dehydration of ethanol on acidic zeolite H-Y.<sup>14</sup> By applying a

stopped-flow protocol<sup>14</sup> similar to those for the in situ preparation<sup>17</sup> of surface methoxy species, surface ethoxy species were observed which gave a  $^{13}\text{C}$  CP/MAS NMR signal at 72.6 ppm accompanied by spinning sidebands characteristic for strongly bound surface species.<sup>14</sup> Formation of surface ethoxy species on acidic zeolite H-Y was further confirmed by an analysis of the chemical shielding tensor and by the reaction of these species with water.<sup>14</sup> In this contribution, the transformation of surface methoxy species to surface ethoxy species and other alkoxy species is shown for the first time, which is achieved by the reaction of surface methoxy species and alkyl halides on acidic zeolite H-Y.

$^{13}\text{C}$  MAS NMR spectroscopy was first applied to investigate the reaction of surface methoxy species ( $^{13}\text{CH}_3\text{-Y}$ ) and  $^{13}\text{C}$ -1-enriched ethyl iodide ( $\text{CH}_3^{13}\text{CH}_2\text{I}$ ). Figure 2a, left, shows the  $^{13}\text{C}$  CP/MAS NMR spectrum recorded after loading of  $\text{CH}_3^{13}\text{CH}_2\text{I}$  on the methylated zeolite Y,  $^{13}\text{CH}_3\text{-Y}$ , at room temperature. The signal at 4 ppm is due to the methylene carbon atoms of the reactant,  $\text{CH}_3^{13}\text{CH}_2\text{I}$ . A weak signal appears at -23 ppm, which is assigned to methyl iodide  $^{13}\text{CH}_3\text{I}$ .<sup>15b</sup> The reaction of surface methoxy species and ethyl iodide becomes more evident at 373 and 423 K, as indicated in Figure 2b and 2c, respectively. A new signal at 73 ppm occurred with spinning sidebands in Figure 2b, left, and dominates the spectrum in Figure 2c, left. In agreement with our recent findings,<sup>14</sup> the signal at 73 ppm is assigned to the methylene carbon atoms of surface ethoxy species,  $\text{CH}_3^{13}\text{CH}_2\text{-Y}$ . The above-mentioned assignments are further supported by the  $^{13}\text{C}$  CP/MAS NMR spectrum shown in Figure 2d, left, which was recorded after the catalyst was hydrated at room temperature. The formation of  $\text{CH}_3^{13}\text{CH}_2\text{OH}$  at 60 ppm and  $^{13}\text{CH}_3\text{OH}$  at 50 ppm indicates the hydrolysis of surface ethoxy species<sup>14</sup> and surface methoxy species<sup>17</sup> by water. The  $^{13}\text{C}$  HPDEC MAS NMR spectra simultaneously recorded for each sample are shown in Figure 2, right. The same signals occur in each  $^{13}\text{C}$  HPDEC MAS NMR spectrum as those in the corresponding  $^{13}\text{C}$  CP/MAS NMR spectrum, although with different relative intensities.

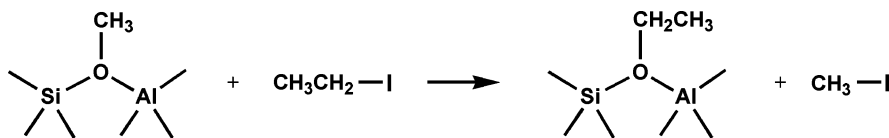
The reaction of surface methoxy species and ethyl iodide is depicted in Scheme 2, which shows the transformation of surface methoxy species to surface ethoxy species on the catalyst. A similar reaction was found for surface methoxy species reacting with other alkyl halides, by which the corresponding alkoxy species are expected to form. Figure 3 shows some representative  $^{13}\text{C}$  HPDEC MAS NMR spectra recorded after the reaction of  $^{13}\text{C}$ -enriched surface methoxy species and nonenriched alkyl halides on zeolite H-Y and silicoaluminophosphate H-SAPO-34. The formation of  $^{13}\text{C}$ -enriched methyl iodide  $^{13}\text{CH}_3\text{I}$  (Figures 3a to 3d) or methyl bromide  $^{13}\text{CH}_3\text{Br}$  (Figure 3e) indicates that the reaction of surface methoxy species and alkyl halides takes place in a similar manner as that described in Scheme 2. For example, after the reaction of  $^{13}\text{C}$ -enriched surface methoxy species ( $^{13}\text{CH}_3\text{-Y}$ ) and nonenriched isopropyl iodide [ $(\text{CH}_3)_2\text{CH-I}$ ] at room temperature, the signal of  $^{13}\text{C}$ -enriched methyl iodide ( $^{13}\text{CH}_3\text{I}$ ) occurs at -23 ppm in the  $^{13}\text{C}$  HPDEC MAS NMR spectrum (Figure 3c). This signal dominates the  $^{13}\text{C}$  HPDEC MAS NMR spectrum after the reaction at 373 K (Figure 3d). Another example is the reaction of  $^{13}\text{C}$ -enriched surface methoxy species and nonenriched ethyl bromide on zeolite H-Y. Figure 3e shows the  $^{13}\text{C}$  HPDEC MAS NMR spectrum recorded after the reaction at 423 K. The



 $^{13}\text{C}$  CP MAS NMR $^{13}\text{C}$  HPDEC MAS NMR

**Figure 2.**  $^{13}\text{C}$  CP/MAS NMR (left) and HPDEC MAS NMR (right) spectra recorded after the reaction of  $^{13}\text{C}$ -1-enriched ethyl iodide ( $\text{CH}_3^{13}\text{CH}_2\text{I}$ , 50 mbar) and surface methoxy species ( $^{13}\text{CH}_3\text{-Y}$ ) at 298 K (a), 373 K (b), 423 K (c). Spectra d show the  $^{13}\text{C}$  MAS NMR spectra recorded after the catalyst sample (c) was hydrated at room temperature. The spinning sidebands of  $^{13}\text{CH}_3\text{-Y}$  are denoted as \*, those of  $\text{CH}_3^{13}\text{CH}_2\text{-Y}$ , as ●, and those of  $\text{CH}_3^{13}\text{CH}_2\text{I}$ , as ■.

#### Scheme 2



dominating signal at 11 ppm, which is due to the  $^{13}\text{C}$ -enriched methyl bromide ( $^{13}\text{CH}_3\text{Br}$ ), indicates the transformation of surface methoxy species to surface ethoxy species by the reaction of surface methoxy species and ethyl bromide on zeolite H-Y. We cannot, however, figure out the detailed mechanism for the reaction of surface methoxy species and alkyl halides. For example, the reaction depicted in Scheme 2 can take place either in one step or in sequential steps which start from the formation of surface ethoxy species and HI, followed by the subsequent reaction of HI with surface methoxy species.

#### Reaction of Surface Methoxy Species and Hydrochloride.

Methyl chloride, which is used as a general methylating agent and as an intermediate in the manufacture of silicones, synthetic rubber, and methyl cellulose, is commercially produced by two

processes: hydrochlorination of methanol and chlorination of methane.<sup>27,28</sup> The hydrochlorination reaction of methanol and hydrochloride, mainly on alumina-based solid catalysts, is usually preferred in industry.<sup>27,28</sup> A recent investigation on the interaction of methanol and  $\eta$ -alumina catalyst shows that chemisorbed methoxy is the only surface species present on the catalyst.<sup>29</sup> Further study indicates that surface methoxy species are involved as a reactive intermediate in hydrochlori-

(27) Makhlin, V. A.; Ivanov, S. I. *Kinet. Catal.* **1997**, *38*, 864–867.

(28) (a) Weissert, K.; Arpe, H. J. In *Industrial Organic Chemistry*, 3rd ed.; VCH: Weinheim, 1997; p 72. (b) Becerra, A. M.; Luna, A. E. C.; Ardisson, D. E.; Ponzi, M. I. *Ind. Eng. Chem. Res.* **1992**, *31*, 1045–1050.

(29) McInroy, A. R.; Lundie, D. T.; Winfield, J. M.; Dudman, C. C.; Jones, P.; Parker, S. F.; Taylor, J. W.; Lennon, D. *Phys. Chem. Chem. Phys.* **2005**, *7*, 3093–3101.

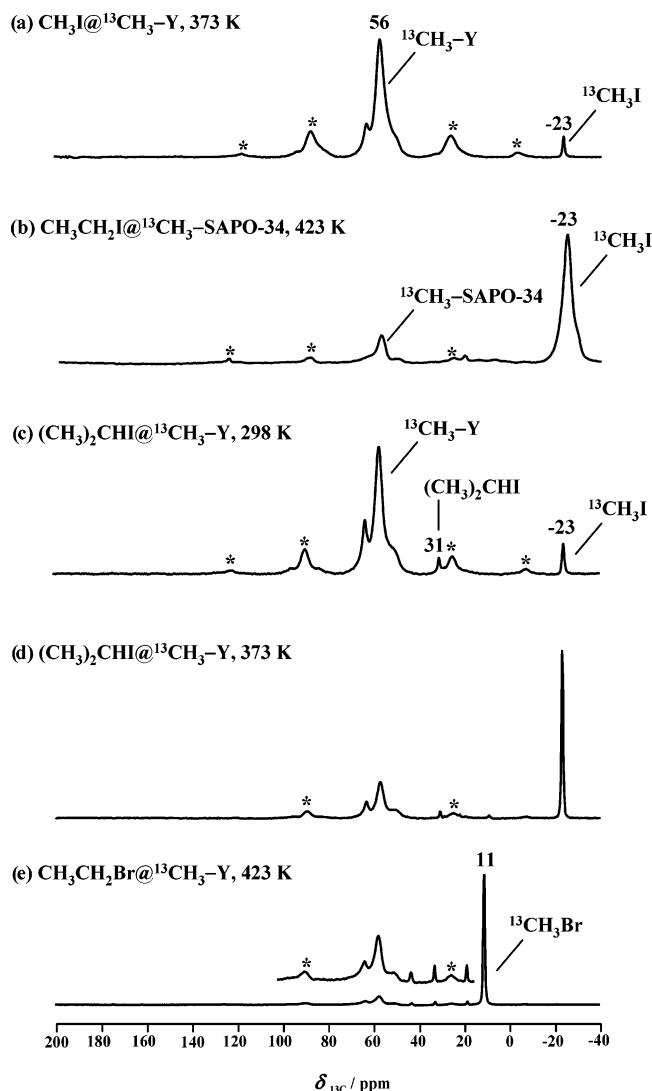


**Figure 3.**  $^{13}\text{C}$  HPDEC MAS NMR spectra recorded after the reaction of methyl iodide ( $\text{CH}_3\text{I}$ , 45 mbar) on methylated zeolite Y ( $^{13}\text{CH}_3\text{-Y}$ ) at 373 K (a), ethyl iodide  $\text{CH}_3\text{CH}_2\text{I}$  (50 mbar) on methylated silicoaluminophosphate SAPO-34 ( $^{13}\text{CH}_3\text{-SAPO-34}$ ) at 423 K (b), isopropyl iodide ( $(\text{CH}_3)_2\text{CHI}$ , 30 mbar) on methylated zeolite Y ( $^{13}\text{CH}_3\text{-Y}$ ) at 298 K (c) and 373 K (d), and ethyl bromide  $\text{CH}_3\text{CH}_2\text{Br}$  (50 mbar) on methylated zeolite Y ( $^{13}\text{CH}_3\text{-Y}$ ) at 423 K (e). Asterisks denote spinning sidebands.

nation of methanol on  $\eta$ -alumina catalyst.<sup>30</sup> Additionally, zeolites have also been suggested as applicable catalysts for the methanol hydrochlorination process.<sup>28,31</sup>

To gain mechanistic information of hydrochlorination of methanol on solid catalysts, the reaction of surface methoxy species and hydrochloride was, therefore, investigated by  $^{13}\text{C}$  MAS NMR spectroscopy. Figure 4a, left, shows the  $^{13}\text{C}$  HPDEC MAS NMR spectrum recorded after the reaction of the methylated catalyst ( $^{13}\text{CH}_3\text{-Y}$ ) and hydrochloride ( $\text{HCl}$ ) at room temperature. As can be seen, a new signal appears at 24 ppm, which is due to the formation of methyl chloride,  $^{13}\text{CH}_3\text{Cl}$ . Upon further reaction at 353 K, the signal of methyl chloride at 24 ppm increases, accompanied by the decrease of the signal of surface methoxy species at 56 ppm (Figure 4b, left). Scheme 3

describes the reaction of surface methoxy species and hydrochloride on zeolite catalyst, by which the Brønsted acidity of the zeolite would be recovered. As a comparison, the reaction of  $^{13}\text{C}$ -enriched methanol and hydrochloride on acidic zeolite  $\text{H-Y}$  was investigated under the same conditions, and the  $^{13}\text{C}$  HPDEC MAS NMR results are shown in Figure 4, right. Similar to the cases of surface methoxy species, the reaction of methanol and hydrochloride on acidic zeolite  $\text{H-Y}$  gives methyl chloride as the product, which is evidenced by the appearance of the  $^{13}\text{C}$  MAS NMR signal of methyl chloride at 24 ppm (Figure 4, right). These results indicate that surface methoxy species may also be involved in methanol hydrochlorination on solid catalysts, which is in agreement with the recent work<sup>30</sup> of Lennon and co-workers, who reported their investigation of methanol hydrochlorination on an  $\eta$ -alumina catalyst by means of temperature programmed reaction spectroscopy (TPRS).

**Koch-Type Carbonylation Reaction: The Reaction of Surface Methoxy Species and Carbon Monoxide.** The classic Koch carbonylation reaction between olefins and carbon monoxide in the presence of water provides evidence for the existence of carbenium ions in superacidic solutions.<sup>32</sup> The first solid-state NMR evidence of the Koch carbonylation reaction on solid acid catalysts was reported in 1995 by Stepanov et al.<sup>33</sup> With the application of  $^{13}\text{C}$  MAS NMR spectroscopy, these authors observed the formation of trimethylacetic acid in high yields upon coadsorption of isobutene, carbon monoxide, and water (or coadsorption of *tert*-butyl alcohol and carbon monoxide) on acidic zeolite  $\text{H-ZSM-5}$  under mild conditions.<sup>33</sup> Based on this discovery, high, stable catalytic performance was recently found for the Koch carbonylation reaction on various solid acid catalysts.<sup>34</sup>

Similar to the case in superacidic solutions,<sup>32</sup> the proposed mechanism (Scheme 4) of Koch carbonylation reaction on acidic zeolites<sup>33,35</sup> involves the trapping of an alkyl carbenium ion ( $\text{R}^+$ , transient species, generated from an olefin or alcohol on an acidic zeolite) by carbon monoxide to form an acylium cation,  $\text{R}-\text{C}^+=\text{O}$ . The latter cation is very unstable and is readily quenched by water to give a carboxylic acid,  $\text{R}-\text{COOH}$ .

As further demonstrated by Stepanov et al.,<sup>36</sup> alkoxy species which possess carbenium-ion-like properties may also follow the Koch carbonylation reaction on acidic zeolites. Fujimoto and co-workers<sup>37</sup> are the first who reported the carbonylation of methanol by carbon monoxide at 473 K on acidic zeolites  $\text{H-Y}$ ,  $\text{H-ZSM-5}$ , and  $\text{H-Mordenite}$ , the main carbonylated products of which are acetic acid ( $\text{CH}_3\text{COOH}$ ) and methyl acetate ( $\text{CH}_3\text{COOCH}_3$ ). The carbonylation reaction of methanol

(30) McInroy, A. R.; Lundie, D. T.; Winfield, J. M.; Dudman, C. C.; Jones, P.; Lennon, D. *4th International Conference on Environmental Catalysis*, 5–8 June, 2005, Heidelberg, Germany. Book of Abstracts, 2005, p 291.  
(31) Magoren. Catalysts for Manufacturing Methyl Chloride. Japanese Patent 58-27644, 1983.

(32) Bahrmann, H. In *New Syntheses with Carbon Monoxide*; Falbe, J., Ed.; Springer-Verlag: Berlin, 1980; p 372.  
(33) (a) Stepanov, A. G.; Luzgin, M. V.; Romannikov, V. N.; Zamaraev, K. I. *J. Am. Chem. Soc.* **1995**, *117*, 3615–3616. (b) Stepanov, A. G.; Luzgin, M. V.; Romannikov, V. N.; Sidelnikov, V. N.; Zamaraev, K. I. *J. Catal.* **1996**, *164*, 411–421.  
(34) (a) Li, T.; Tsumori, N.; Souma, Y.; Xu, Q. *Chem. Commun.* **2003**, 2070–2071. (b) Tsumori, N.; Xu, Q.; Souma, Y.; Mori, H. *J. Mol. Catal. A: Chem.* **2002**, *179*, 271–277. (c) Xu, Q.; Inoue, S.; Tsumori, N.; Mori, H.; Kameda, M.; Tanaka, M.; Fujiwara, M.; Souma, Y. *J. Mol. Catal. A: Chem.* **2001**, *170*, 147–153. (d) Mori, H.; Wada, A.; Xu, Q.; Souma, Y. *Chem. Lett.* **2000**, 136–137.  
(35) (a) Luzgin, M. V.; Romannikov, V. N.; Stepanov, A. G.; Zamaraev, K. I. *J. Am. Chem. Soc.* **1996**, *118*, 10890–10891. (b) Clingenpeel, T. H.; Wessel, T. E.; Biaglow, A. I. *J. Am. Chem. Soc.* **1997**, *119*, 5469–5470. (c) Clingenpeel, T. H.; Biaglow, A. I. *J. Am. Chem. Soc.* **1997**, *119*, 5077–5078.  
(36) Stepanov, A. G.; Luzgin, M. V.; Romannikov, V. N.; Sidelnikov, V. N.; Paukshtis, E. A. *J. Catal.* **1998**, *178*, 466–477.  
(37) Fujimoto, K.; Shikada, T.; Omata, K.; Tominaga, H. *Chem. Lett.* **1984**, 2047–2050.

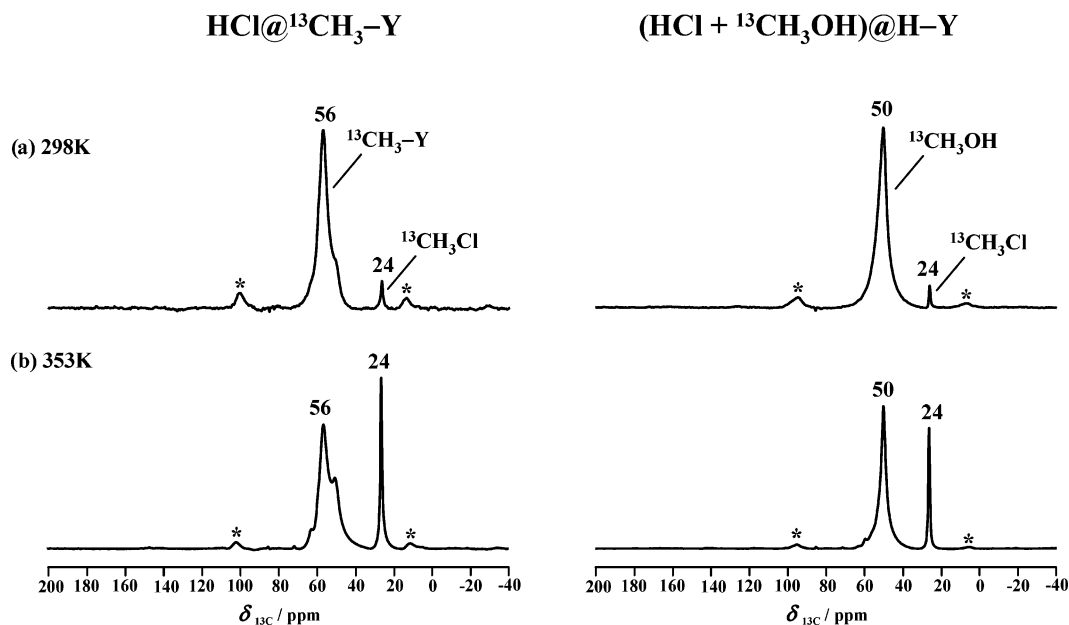
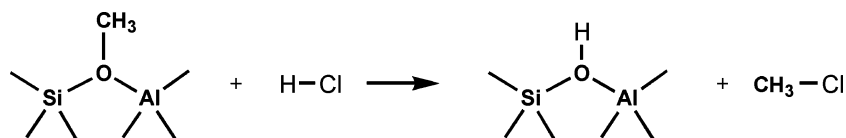
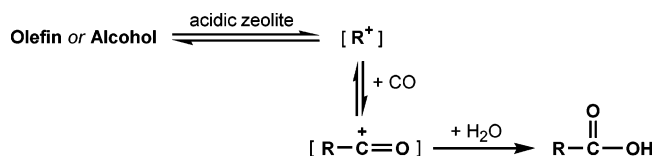


**Figure 4.**  $^{13}\text{C}$  HPDEC MAS NMR spectra recorded after the reaction of hydrochloride (HCl, 50 mbar) on methylated zeolite Y ( $^{13}\text{CH}_3\text{-Y}$ ) (left) and after the reaction of methanol (50 mbar) and hydrochloride (50 mbar) on acidic zeolite H-Y (right) at 298 K (a) and 353 K (b), respectively. Asterisks denote spinning sidebands.

#### Scheme 3

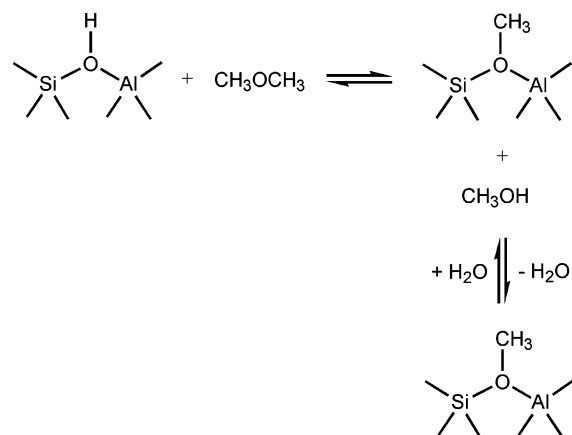


#### Scheme 4



on acid zeolites was proposed<sup>37</sup> to follow the Koch reaction shown in Scheme 4, with the formation of surface methoxy species as the key intermediate. A similar pathway, which involves the reaction of surface methoxy species and carbon monoxide, was also suggested recently by Iglesia and co-workers for the carbonylation reaction of dimethyl ether on acidic zeolites.<sup>38</sup> The suggestion of Iglesia and co-workers<sup>38</sup> is verified by our  $^{13}\text{C}$  MAS NMR investigations presented in this contribution. Figure 5a shows the  $^{13}\text{C}$  CP/MAS NMR spectrum recorded after the reaction of  $^{13}\text{C}$ -enriched carbon monoxide ( $^{13}\text{CO}$ ) and nonenriched dimethyl ether (DME,  $\text{CH}_3\text{OCH}_3$ ) on acidic zeolite H-Y at 473 K. In agreement with previous findings,<sup>33,38,39</sup> the  $^{13}\text{C}$  MAS NMR signal at 184 ppm with characteristic spinning sidebands is assigned to the carbonyl carbon of acetic acid,  $\text{CH}_3^{13}\text{COOH}$ . This assignment was further supported by the adsorption of  $\text{CH}_3^{13}\text{COOH}$  on zeolite H-Y. The  $^{13}\text{C}$  CP/MAS NMR recorded thereafter shows the identical chemical shift and very similar spinning sidebands as observed for the signal at 184 ppm in Figure 5a. On the other hand,  $^{13}\text{CO}$  which also has the  $^{13}\text{C}$  chemical shift of ca. 184 ppm<sup>33</sup> is only weakly adsorbed on zeolite H-Y and does not show any appreciable signal in the  $^{13}\text{C}$  CP/MAS NMR spectrum (not

#### Scheme 5



shown). As a control experiment, Figure 5b shows the  $^{13}\text{C}$  CP/MAS NMR spectrum recorded after the reaction of nonenriched DME on acidic zeolite H-Y at 473 K. The signals at 63 and 60 ppm are due to side-on and end-on adsorbed DME, respectively.<sup>17</sup> The signals appearing at 56 and 50 ppm indicate the reversible formation of surface methoxy species and methanol by the decomposition of DME on acidic zeolites at high temperatures, which agrees well with the work of Iglesia and co-workers<sup>38</sup> and of Forester and Howe.<sup>16</sup> The formation of surface methoxy species, methanol, and water upon the decomposition of DME is, accordingly, depicted in Scheme 5. Therefore, the above-mentioned results provide the first  $^{13}\text{C}$  MAS NMR evidence for the mechanism of the carbonylation reaction of

(38) Cheung, P. C.; Bhan, A.; Sunley, G. L.; Iglesia, E. *Angew. Chem., Int. Ed.* **2006**, *45*, 1617–1620.

(39) Kresnawahjuesa, O.; Gorte, R. J.; White, D. J. *Mol. Catal. A: Chem.* **2004**, *208*, 175–185.

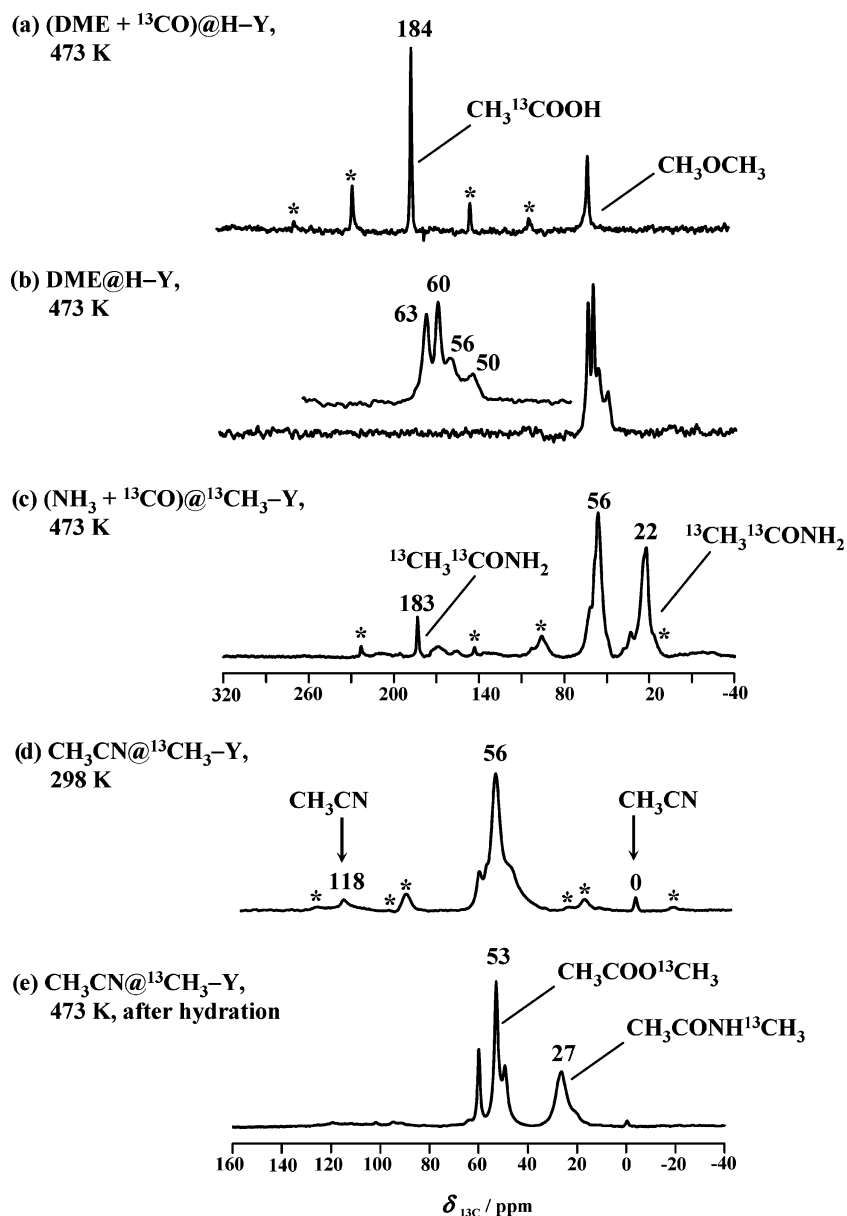
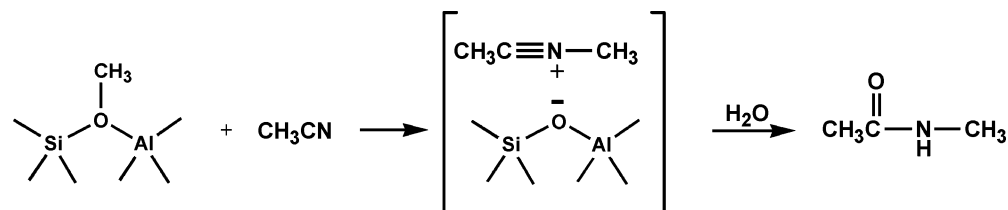


**Figure 5.**  $^{13}\text{C}$  CP/MAS NMR spectra recorded after the reaction of dimethyl ether (DME, 40 mbar) and  $^{13}\text{CO}$  (35 mbar) at 473 K on acidic zeolite H-Y (a), after the reaction of DME (110 mbar) at 473 K on acidic zeolite H-Y (b), and after the reaction of ammonia (38 mbar) and  $^{13}\text{CO}$  (45 mbar) on methylated zeolite Y ( $^{13}\text{CH}_3\text{-Y}$ ) at 473 K. Spectra d and e show the  $^{13}\text{C}$  HPDEC MAS NMR spectra recorded after the reaction of acetonitrile (50 mbar) on methylated zeolite Y ( $^{13}\text{CH}_3\text{-Y}$ ) at 298 K (a) and 473 K (b), respectively. Asterisks denote spinning sidebands.

#### Scheme 6



dimethyl ether by carbon monoxide on acidic zeolites, which was originally proposed<sup>38</sup> by Iglesia and co-workers. In agreement with previous work,<sup>33</sup> the formation of an unstable acylium cation,  $\text{CH}_3\text{-C}^+=\text{O}$ , by the reaction of surface methoxy species and CO, was not directly observed by  $^{13}\text{C}$  MAS NMR spectroscopy. However, the transient existence of this cation was further evidenced by our trapping experiment with ammonia, the idea of which was originally presented in the work of Gorte

and co-workers.<sup>39</sup> Figure 5c shows the  $^{13}\text{C}$  CP/MAS NMR spectrum recorded after the reaction of  $^{13}\text{C}$ -enriched carbon monoxide, ammonia, and the methylated catalyst,  $^{13}\text{CH}_3\text{-Y}$ , at 473 K. The formation of acetamide,  $^{13}\text{CH}_3^{13}\text{CONH}_2$ , is evidenced by the  $^{13}\text{C}$  signals at 22 ppm for the methyl carbon and 183 ppm for the carbonyl carbon, respectively. This finding indicates the trapping of the unstable acylium cation,  $\text{CH}_3\text{-C}^+=\text{O}$ , with ammonia, by which the stable product acetamide is formed. Our



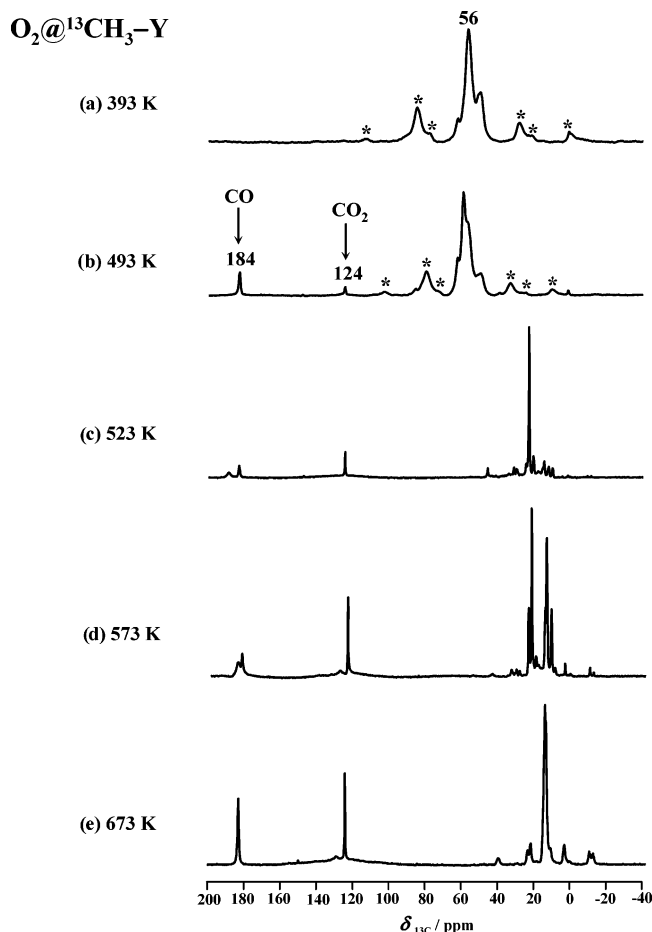


**Figure 6.**  $^{13}\text{C}$  HPDEC MAS NMR spectra recorded after thermal treatments of methylated zeolite Y ( $^{13}\text{CH}_3\text{-Y}$ ) in the presence of oxygen (ca. 5 mbar) at elevated temperatures of 393 (a) to 673 K (e). Asterisks denote spinning sidebands.

result agrees well with the previous work of Gorte and co-workers,<sup>39</sup> who observed the formation of acetamide from the reaction of ammonia and the acylium cation on zeolite H-ZSM-5 by TPD-TGA measurements.

**Ritter-Type Reaction: The Reaction of Surface Methoxy Species and Acetonitrile.** Stepanov and Luzgin<sup>40</sup> investigated the reaction of acetonitrile with olefins (1-octene) or alcohols (*tert*-butyl alcohol) on acidic zeolite H-ZSM-5. In the case of acetonitrile and alcohol coadsorbed on zeolite H-ZSM-5 at room temperature, the intermediate N-alkylnitrilium cation and the final product N-alkylamide are observed simultaneously by MAS NMR spectroscopy.<sup>40</sup> The experimental results were rationalized in accordance with the classic Ritter reaction.<sup>40</sup> Surface alkoxy species react with acetonitrile to produce the intermediate of the N-alkylnitrilium cation, which can be further hydrolyzed to form N-alkylamide as the final product.<sup>40</sup>

In this contribution, the reaction of surface methoxy species and acetonitrile on zeolite Y was investigated by  $^{13}\text{C}$  MAS NMR spectroscopy. Figure 5d shows the  $^{13}\text{C}$  HPDEC MAS NMR spectrum recorded after nonenriched acetonitrile ( $\text{CH}_3\text{CN}$ ) was loaded onto the methylated zeolite Y ( $^{13}\text{CH}_3\text{-Y}$ ) at room temperature. Besides the signal of surface methoxy species at 56 ppm in Figure 5d, two weak signals of acetonitrile occur at 118 and 0 ppm, respectively. No reaction can be observed at

this temperature. Upon thermal treatment of the catalyst sample at 473 K for 20 min and subsequent hydrolysis, the  $^{13}\text{C}$  HPDEC MAS NMR spectrum recorded is shown in Figure 5e. The broad signal at 27 ppm in Figure 5e is due to the formation of *N*-methyl acetamide,  $\text{CH}_3\text{CONH}^{13}\text{CH}_3$ . The broadening of this signal is typically caused by the  $^{13}\text{C}\text{--}^{14}\text{N}$  dipolar coupling, which is strongly affected by the quadrupolar  $^{14}\text{N}$  nuclei.<sup>41</sup> In agreement with Stepanov and Luzgin,<sup>40</sup> the formation of *N*-methyl acetamide observed in Figure 5d is depicted in Scheme 6. The additional signal occurring at 53 ppm in Figure 5e is assigned to methyl acetate,  $\text{CH}_3\text{COO}^{13}\text{CH}_3$ . The formation of methyl acetate is caused by the reaction of surface methoxy species with acetic acid. The latter species can be formed by the hydrolysis of acetonitrile on acidic zeolites.<sup>40</sup>

**Oxidation of Surface Methoxy Species.** Recent  $^{13}\text{C}$  MAS NMR investigations indicate that the decomposition of surface methoxy species at reaction temperatures of ca. 523 K and higher results in the formation of hydrocarbons on acidic zeolite catalysts.<sup>17c,d</sup> Hutchings and co-workers<sup>42</sup> are the first who investigated the conversion of methanol or DME at 573 K on acidic zeolite H-ZSM-5 in the presence of oxygen. It was found that the zeolite catalysts in their fixed-bed reactor were irreversibly deactivated, especially at higher oxygen concentrations.<sup>42</sup> The effect of oxygen cofeeding was explained by the formation of formic acid and formaldehyde, the latter of which would undergo polymerization in strong acidic media.<sup>42</sup> In this contribution, the influence of low concentration of oxygen on the decomposition of surface methoxy species was investigated by  $^{13}\text{C}$  MAS NMR spectroscopy. Figure 6 shows the  $^{13}\text{C}$  HPDEC MAS NMR spectra recorded after thermal treatments of the methylated catalyst,  $^{13}\text{CH}_3\text{-Y}$ , in the presence of oxygen (ca. 5 mbar). Carbon monoxide and carbon dioxide are formed at ca. 493 K, which give  $^{13}\text{C}$  MAS NMR signals at 184 and 124 ppm, respectively (Figure 6b to 6e). In agreement with our previous findings,<sup>17c,d</sup> the decomposition of surface methoxy species to hydrocarbons starts at ca. 523 K, as indicated in Figure 6c. The hydrocarbons formed in this case (Figures 6c to 6e) are essentially identical to those in the absence of oxygen (Figure 4 in ref 17c).

It is important to note that the formation of carbon monoxide and carbon dioxide (Figure 6b) starts earlier than the onset of the decomposition of surface methoxy species to hydrocarbons. In agreement with Hutchings and co-workers,<sup>42</sup> our NMR results of the oxidation of surface methoxy species by oxygen (Figure 6) are interpreted as the formation of formaldehyde and formic acid which further decompose to carbon monoxide and carbon dioxide. Carbon monoxide is neither an intermediate nor a catalyst during the MTO process, as clarified by Haw and co-workers.<sup>43</sup> Therefore, in the presence of oxygen, the oxidation of surface methoxy species compete with the thermal decomposition of surface methoxy species. However, oxygen may not play an active role to initiate the formation of primary

(40) Stepanov, A. G.; Luzgin, M. V. *Chem.-Eur. J.* **1997**, *3*, 47–56.

(41) Naito, A.; Ganapathy, S.; McDowell, C. A. *J. Chem. Phys.* **1981**, *74*, 5393–5397.  
 (42) (a) Hunter, R.; Hutchings, G. J.; Pickl, W. *J. Chem. Soc., Chem. Commun.* **1987**, 1369–1371. The effect of oxygen cofeeding on the conversion of methanol or dimethyl ether on acidic zeolites was discussed in: (b) Hutchings, G. J.; Hunter, R. *Catal. Today* **1990**, *6*, 279–306. (c) Hutchings, G. J.; van Rensburg, L. J.; Pickl, W.; Hunter, R. *J. Chem. Soc., Faraday Trans. 1* **1988**, *84*, 1311–1328.  
 (43) Munson, E. J.; Lazo, N. D.; Moellenhoff, M. E.; Haw, J. F. *J. Am. Chem. Soc.* **1991**, *113*, 2783–2784.

hydrocarbons in the MTO process, as implied in the previous work of Hutchings and co-workers<sup>42</sup> and in the present study.

## Discussion

Intermediates involved in heterogeneously catalyzed reactions can vary in nature from highly reactive species to relatively unreactive ones. In either case, the lifetime of the intermediates must be long enough for successful detection by the spectroscopic method being applied. Similar to the strategy achieved in solution chemistry, it is also possible to further isolate the long-lived intermediates formed in some heterogeneously catalyzed systems and investigate independently their nature and chemical reactivity thereafter. This approach is exemplified in the present contribution where the isolation of surface methoxy species on acidic zeolites can be followed by further investigations of their reactivity with probe molecules. In this section, the stability and reactivity of surface methoxy species are further discussed in comparison with those of other surface alkoxy species ( $> C_1$  species).

Carbenium ions are key intermediates involved in a variety of acid-catalyzed reactions performed in solution.<sup>1,2</sup> Due to the low dielectric constants of acidic zeolites and the absence of solvation effects in zeolites,<sup>4b,10e</sup> however, simple carbenium ions may exist as highly activated and short-lived transition states and, therefore, only represent saddle points on the potential energy surface.<sup>4,7,8a</sup> Indeed, persistent carbenium ions experimentally identified in zeolites are mainly bulky cyclic cations which are charge-delocalized in nature and sterically hindered to the negatively charged zeolite framework.<sup>44</sup> On the other hand, covalent alkoxy species<sup>3–6,14</sup> have been consistently observed as long-lived intermediates upon the adsorption of small olefins or dehydration of simple alcohols on acidic zeolites. In 1989, Gorte and co-workers<sup>4a</sup> first identified by <sup>13</sup>C NMR spectroscopy the formation of surface *tert*-butoxy species upon the adsorption of *tert*-butyl alcohol on acidic zeolite H-ZSM-5. Later in the same year, Haw and co-workers<sup>6a</sup> reported the <sup>13</sup>C CP/MAS NMR evidence for surface isopropoxy species formed from the reaction of propene on acidic zeolite H-Y. Subsequently, Stepanov et al. detected by <sup>13</sup>C NMR spectroscopy the formation of surface isobutoxy species upon the conversion of isobutanol<sup>5</sup> and the formation of oligomeric alkoxy species upon adsorption of ethene,<sup>36</sup> both on acidic zeolite H-ZSM-5. The IR investigations on the formation of oligomeric alkoxy species upon adsorption of ethene and propene on acidic zeolites H-ZSM-5 and H-Mordenite were reported by Zecchina and co-workers.<sup>45</sup> Adding to the rare evidence for the existence of surface alkoxy species ( $> C_1$  species), surface ethoxy species formed from ethanol was recently observed on acidic zeolites H-Mordenite<sup>3b</sup> and H-Y,<sup>14</sup> respectively. The reactivity and the carbenium-ion-like nature of surface alkoxy intermediates formed in acidic zeolites were addressed in the pioneering work of Gorte and co-workers.<sup>4</sup> Nevertheless, knowledge on the reactivity of surface alkoxy species ( $> C_1$  species) is still severely lacking so far, largely due to the occurrence of rapid secondary reactions on the solid catalysts which hindered the isolation of primary intermediates and complicates the interpretation of experimental results.

In contrast, surface methoxy species, i.e., the simplest form and probably the most stable form of surface alkoxy species, have been extensively investigated, mostly in connection with mechanistic studies of methanol-to-hydrocarbon conversion<sup>46</sup> on solid acids. Table 1 summarizes typical IR and NMR evidence for the formation of surface methoxy species upon the reactions of methanol on various solid acids. Despite the unequivocal observation of surface methoxy species on solid acids, the role of these surface methoxy species in heterogeneous catalysis has been disputed in a controversial manner. The reactivity of surface methoxy species in acidic zeolites may be better discussed in terms of C–O bond and C–H bond activation, respectively. The C–O bond reactivity of surface methoxy species has been evidenced by reactions with various probe molecules, some of which are included in Table 1. For example, surface methoxy species on acidic zeolites can react with water<sup>17c,53</sup> to produce methanol at room temperature, with methanol<sup>17a,52</sup> to form DME, with aniline<sup>23,24</sup> to form *N*-methylanilinium cations, with benzene<sup>16,48,50,53</sup> or toluene<sup>17c</sup> to form alkyl-substituted aromatics (such as, toluene, xylenes, and ethylbenzenes) and react with ethene<sup>16,55b</sup> or propene<sup>16</sup> to reproduce olefins which may undergo further oligomerization reactions.<sup>16</sup> Our results in this contribution further indicate that surface methoxy species can react with ammonia, alkyl halides, hydrochloride, carbon monoxide (Koch-type carbonylation reaction), and acetonitrile (Ritter-type reaction). Therefore, surface methoxy species act as an effective methylating agent in a variety of reactions with probe molecules on solid acids, in which the C–O bond activation of surface methoxy species is involved.

The relative reactivity of surface alkoxy species in terms of C–O bond activation can be evaluated by benefit of recent theoretical investigations<sup>7–13</sup> of olefin adsorption on acidic zeolites. As depicted in Figure 7, the adsorption of small olefins on acidic zeolites starts with the formation of a  $\pi$ -complex (**2A** for ethene, **3A** for propene, and **4A** for isobutene in Figure 7), and through a transition state which most probably involves carbenium cations (**2B**, **3B**, and **4B** in Figure 7), the corresponding surface alkoxy species ( $\sigma$ -complex, **2C**, **3C**, and **4C** in Figure 7) are formed. Although the energy difference of species in Figure 7 cannot be quantitatively compared, the basic trends for their relative stability are evident. For example, theoretical calculations<sup>9a,9b,10d,59</sup> predict that the relative stability of surface alkoxy species being formed upon adsorption of

- (44) Hunger, M.; Wang, W. *Adv. Catal.* **2006**, *50*, 149–225.  
 (45) (a) Spoto, G.; Bordiga, S.; Ricchiardi, G.; Scarano, D.; Zecchina, A.; Borello, E. *J. Chem. Soc., Faraday Trans.* **1994**, *90*, 2827–2835. (b) Geobaldo, F.; Spoto, G.; Bordiga, S.; Lamberti, C.; Zecchina, A. *J. Chem. Soc., Faraday Trans.* **1997**, *93*, 1243–1249.

- (46) Stöcker, M. *Microporous Mesoporous Mater.* **1999**, *29*, 3–48.  
 (47) Salvador, P.; Kladnig, W. *J. Chem. Soc., Faraday Trans. 1* **1977**, *73*, 1153–1168.  
 (48) Ono, Y.; Mori, T. *J. Chem. Soc., Faraday Trans. 1* **1981**, *77*, 2209–2221.  
 (49) (a) Novakova, J.; Kubelkova, L.; Dolejšek, Z. *J. Catal.* **1987**, *108*, 208–213. (b) Kubelkova, L.; Novakova, J.; Nedomova, K. *J. Catal.* **1990**, *124*, 441–450.  
 (50) Rakoczy, J.; Romotowski, T. *Zeolites* **1993**, *13*, 256–260.  
 (51) Benito, P. L.; Gayubo, A. G.; Aguayo, A. T.; Olazar, M.; Bilbao, J. *J. Chem. Technol. Biotechnol.* **1996**, *66*, 183–191.  
 (52) Wakabayashi, F.; Kondo, J. N.; Hirose, C.; Domen, K. Proceedings of the 12th International Zeolite Conference; Treacy, M. M. J., Marcus, B. K., Bisher, M. E., Higgins, J. B., Eds.; Materials Research Society: Warrendale, 1999; pp 2577–2584.  
 (53) Datka, J.; Rakoczy, J.; Zadrozna, G. Proceedings of the 12th International Zeolite Conference, Materials Research Society; Treacy, M. M. J., Marcus, B. K., Bisher, M. E., Higgins, J. B., Eds.; Materials Research Society: Warrendale, 1999; pp 2601–2608.  
 (54) Derouane, E. G.; Gilson, J. P.; Nagy, J. B. *Zeolites* **1982**, *2*, 42–46.  
 (55) (a) Salehirad, F.; Anderson, M. W. *J. Catal.* **1998**, *177*, 189–207. (b) Salehirad, F.; Anderson, M. W. *J. Catal.* **1996**, *164*, 301–314.  
 (56) Salehirad, F.; Anderson, M. W. *J. Chem. Soc., Faraday Trans.* **1998**, *94*, 2857–2866.

**Table 1.** Experimental Observations of Surface Methoxy Species Formed from Methanol on Solid Acid Catalysts

solid acid	reactant	assignments of surface methoxy species and additional observations	ref
H-ZSM-5 ( $n_{\text{Si}}/n_{\text{Al}} = 15, 26$ )	$\text{CH}_3\text{OH}$ , $\text{CD}_3\text{OH}^a$	IR bands: 2980, 2868, and $1460\text{ cm}^{-1}$ ( $\text{CH}_3$ -ZSM-5); responsible for the methylation of olefins and benzene at 523 K; the onset of significant hydrocarbon formation is accompanied by the cleavage of C–D bonds in $\text{CD}_3$ -ZSM-5 above 523 K.	16
H-Y ( $n_{\text{Si}}/n_{\text{Al}} = 1.9$ , 86% exchange degree)	$\text{CH}_3\text{OH}^b$	IR bands: $2800\text{--}3100\text{ cm}^{-1}$ ( $\text{CH}_3$ -Y); secondary reactions take place above 513 K with the formation of hydrocarbons.	47
H-ZSM-5 ( $n_{\text{Si}}/n_{\text{Al}} = 17.8$ )	$\text{CD}_3\text{OH}^b$	IR bands: 2220 and $2070\text{ cm}^{-1}$ ( $\text{CD}_3$ -ZSM-5); stable up to 512 K; desorption of surface methoxy groups is accompanied by the cleavage of C–D bonds.	48
H-Y ( $n_{\text{Si}}/n_{\text{Al}} = 2.5$ , 70% exchange degree) dealuminated H-Y ( $n_{\text{Si}}/n_{\text{Al}} = 12$ )	$\text{CH}_3\text{OH}^b$	IR bands: $2855\text{--}3000$ and $2855\text{ cm}^{-1}$ ; highly reactive above 573 K and readily participate in the formation of C–C bonds at 523–623 K.	49 <sup>c</sup>
H-ZSM-5 ( $n_{\text{Si}}/n_{\text{Al}} = 14, 18, 19$ )	$\text{CH}_3\text{OH}$ , $\text{CD}_3\text{OD}^b$	IR bands: 2980 and $2850\text{ cm}^{-1}$ ( $\text{CH}_3$ -Y), 2130 and $2070\text{ cm}^{-1}$ ( $\text{CD}_3$ -Y); reaction with benzene at 533 K and decomposition above 581 K.	50
H-ZSM-5 ( $n_{\text{Si}}/n_{\text{Al}} = 24, 42, 78, 154$ )	$\text{CH}_3\text{OH}^b$	IR bands: 2980, 2959, and $2855\text{ cm}^{-1}$ ( $\text{CH}_3$ -ZSM-5); decomposition above 573 K.	51
H-ZSM-5 ( $n_{\text{Si}}/n_{\text{Al}} = 27$ )	$\text{CH}_3\text{OH}^b$	IR bands: $2856\text{--}2978\text{ cm}^{-1}$ ( $\text{CH}_3$ -ZSM-5); involved in the dehydration of methanol to DME at 493 K.	52 <sup>c</sup>
H-X ( $n_{\text{Si}}/n_{\text{Al}} = 1.1$ , 40% exchange degree)	$\text{CH}_3\text{OH}^b$	IR bands: $2968\text{ cm}^{-1}$ ( $\text{CH}_3$ -X) and $2977\text{ cm}^{-1}$ ( $\text{CH}_3$ -Y); responsible for benzene methylation; decomposition at 570 K with the formation of hydrocarbons.	53
H-Y ( $n_{\text{Si}}/n_{\text{Al}} = 2.6$ , 40% and 77% exchange degree)	$\text{CH}_3\text{OH}$ + $\text{NH}_3^c$	IR bands: $2957$ and $2855\text{ cm}^{-1}$ ( $\text{CH}_3$ -ZSM-5).	22
H-ZSM-5 ( $n_{\text{Si}}/n_{\text{Al}} = 35$ )	$^{13}\text{CH}_3\text{OH}^b$	$^{13}\text{C}$ MAS NMR signals: 56 ppm ( $^{13}\text{CH}_3$ -Y), 59.4 ppm ( $^{13}\text{CH}_3$ -ZSM-5).	15
H-ZSM-5 ( $n_{\text{Si}}/n_{\text{Al}} = 22$ )	$^{13}\text{CH}_3\text{OH}^{b,c}$	$^{13}\text{C}$ MAS NMR signals: 56.2 ppm ( $^{13}\text{CH}_3$ -Y), 59.2 ppm to ( $^{13}\text{CH}_3$ -ZSM-5), 56.6 ppm ( $^{13}\text{CH}_3$ -SAPO-34); react with water to methanol, with methanol to DME, with toluene to xylenes; decomposition at 523 K, responsible for the formation of hydrocarbons and for the methylation of cyclohexane.	17
H-Y ( $n_{\text{Si}}/n_{\text{Al}} = 2.7$ , 90% exchange degree)			
H-ZSM-5 ( $n_{\text{Si}}/n_{\text{Al}} = 22$ )			
H-SAPO-34 [ $n_{\text{Si}}/(n_{\text{Al}} + n_{\text{Si}} + n_{\text{P}}) = 0.11$ ]	$^{13}\text{CH}_3\text{OH}$ + aniline <sup>b</sup>	$^{13}\text{C}$ MAS NMR signals: 56 ppm ( $^{13}\text{CH}_3$ -Y); responsible for aniline methylation at 373 to 523 K.	23
H-Y ( $n_{\text{Si}}/n_{\text{Al}} = 2.6$ )	$^{13}\text{CH}_3\text{OH}^b$	$^{13}\text{C}$ MAS NMR signals: 59.9 ppm ( $^{13}\text{CH}_3$ -ZSM-5), 60.7 ppm ( $^{13}\text{CH}_3$ -mordenite).	54
H-ZSM-5 ( $n_{\text{Si}}/n_{\text{Al}} = 19, 26$ )			
H-mordenite ( $n_{\text{Si}}/n_{\text{Al}} = 9$ )	$^{13}\text{CH}_3\text{OH}^b$	$^{13}\text{C}$ MAS NMR signals: 53–59 ppm ( $^{13}\text{CH}_3$ -ZSM-5), 57 ppm ( $^{13}\text{CH}_3$ -SAPO-34).	55
H-SAPO-34 ( $n_{\text{Si}}/n_{\text{Al}} = 0.17$ )			
H-ZSM-5 ( $n_{\text{Si}}/n_{\text{Al}} = 28, 36, 40$ )	$^{13}\text{CH}_3\text{OH}^b$	$^{13}\text{C}$ MAS NMR signals: 56–62 ppm; form at the onset of hydrocarbon formation.	56
H-ZSM-23 ( $n_{\text{Si}}/n_{\text{Al}} = 35$ )			
H-SAPO-11 ( $n_{\text{Si}}/n_{\text{Al}} = 0.25$ )			
H-SAPO-5 ( $n_{\text{Si}}/n_{\text{Al}} = 0.25$ )	$^{13}\text{CH}_3\text{OH}^d$	$^{13}\text{C}$ MAS NMR signals: 56 ppm ( $^{13}\text{CH}_3$ -SAPO-34); decreases dramatically in the first 30 s during which the initiation reaction of MTO catalysis takes place.	57
H-SAPO-34 (1.1 mmol SiOHAl per gram)		$^{13}\text{C}$ MAS NMR signals: 59 ppm; formation of surface methoxy species and hydrocarbons is observed 2 s after methanol injection.	58
sulfated zirconia	$^{13}\text{CH}_3\text{OH}^d$		

<sup>a</sup> In situ IR cell as a pulse microreactor. <sup>b</sup> Batchlike conditions; adsorption and evacuation. <sup>c</sup> Flow conditions. <sup>d</sup> Pulse-quench experiment. <sup>e</sup> IR bands of surface methoxy species summarized therein.

corresponding olefins on acidic zeolites follows the order ethoxy (**2C**) > isopropoxy (**3C**) > *tert*-butoxy (**4C**). On the other hand, it is well-known that primary carbenium-ion-like transition states present much higher activation energies than tertiary carbenium-

ion-like transition states, which results in the relative stability of carbenium ions in the order **4B** > **3B** > **2B** in Figure 7, assuming that the energies for the corresponding  $\pi$ -complex (**2A**, **3A**, and **4A** in Figure 7) do not have much difference. In contrast to the cases of alkoxy species (> C<sub>1</sub> species) formed from olefin

(57) Song, W.; Haw, J. F.; Nicholas, J. B.; Heneghan, C. S. *J. Am. Chem. Soc.* **2000**, *122*, 10726–10727.

(58) Sassi, A.; Song, W.; Wildman, M. A.; Haw, J. F. *Catal. Lett.* **2002**, *81*, 101–105.

(59) Sinclair, P. E.; de Vries A.; Sherwood, P.; Catlow, C. R. A.; van Santen, R. A. *J. Chem. Soc., Faraday Trans.* **1998**, *94*, 3401–3408.

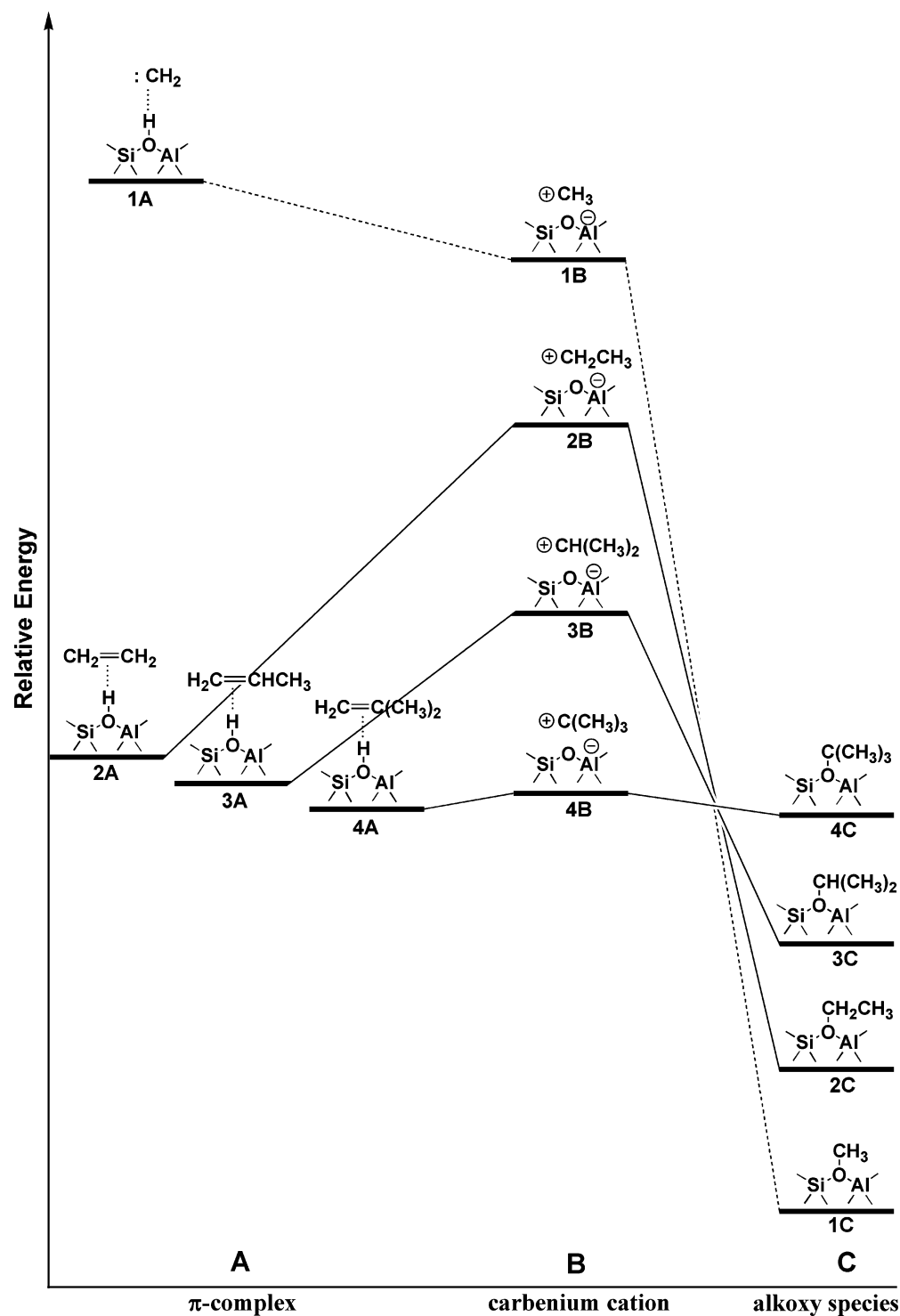


**Figure 7.** Energy profile for the formation of surface alkoxy species derived from recent theoretical investigations.<sup>7–13</sup>

adsorption on acidic zeolites, theoretical calculations have been dealing with the formation of surface methoxy species from dehydration of methanol only, which makes the systematic comparison complicated. Nevertheless, it is still reasonable to add methoxy species (**1C**) as the most stable alkoxy species and, accordingly, methyl cations (**1B**) as the most unstable carbenium cations in Figure 7. The reactivity of surface alkoxy species in terms of C–O bond activation can be, therefore, discussed by looking into the energy differences from **C** to **B** in Figure 7, which are directly related to the activation energies

being considered. The following results may be derived: (i) According to the Hammond Postulate,<sup>60</sup> the surface *tert*-butoxy species would possess more carbenium-ion-like nature than other alkoxy species presented in Figure 7. On the contrary, the covalent-bond nature is more profound in the case of surface methoxy species. Indeed, theoretical calculations<sup>8b</sup> do indicate that the C–O bond distances decrease in the order tertiary >

(60) Hammond, G. S. *J. Am. Chem. Soc.* **1955**, *77*, 334–338. For discussion of the Hammond Postulate, for example, see: Farcasiu, D. *J. Chem. Educ.* **1975**, *52*, 76–79.



secondary > primary alkoxide from 163 to 150 pm. (ii) The nucleophilic substitution reaction with surface methoxy species is more  $S_N2$ -mechanism oriented, which means that the reaction is achieved in a single step and both nucleophile (probe molecules) and surface methoxy species take part in the transition state. The involvement of probe molecules in the transition state will, more or less, decrease the activation energy in comparison with the energy difference between **1C** and **1B** in Figure 7. This explains why the reactions of surface methoxy species with probe molecules having high nucleophilicity (water, ammonia or methylamines) take place at room temperature, while with low nucleophilicity (hydrochloride, carbon monoxide, or acetonitrile) higher reaction temperatures are required. On the contrary, the  $S_N1$  mechanism may dominate the nucleophilic substitution reaction of the bulky *tert*-butoxy species on acidic zeolites. In this case, the presence of probe molecules does not contribute significantly in the rate-determining step in which the transition state largely resembles free carbenium ions, and therefore, the activation energy in this step should be close to the energy difference between **4C** and **4B** shown in Figure 7.

A further issue is the C–H bond activation of surface methoxy species in the absence of other reactants and at reaction temperatures higher than ca. 523 K. This topic is directly related to mechanistic investigations of the first C–C bond formation in the MTO process.<sup>46</sup> Some of experimental observations on the C–H bond activation of surface methoxy species are summarized in Table 1. For example, Ono and Mori<sup>48</sup> reported the IR evidence for the formation of surface methoxy groups on zeolite H–ZSM-5 from  $CD_3OH$  and showed that the desorption of methoxy species from the catalyst is accompanied by the cleavage of C–D bonds at temperatures higher than 512 K. By in situ IR spectroscopy, Forester and Howe<sup>16</sup> observed that the onset of significant hydrocarbon formation is correlated with the cleavage of C–D bonds in  $CD_3$ –ZSM-5 above 523 K. Datka et al.<sup>53</sup> found that the decomposition of surface methoxy species on zeolites H–X and H–Y results in the formation of  $C_2$ – $C_5$  olefins and a small amount of alkanes. They proposed that disproportionation of olefins would form alkanes and aromatics (coke, IR bands at  $1590\text{ cm}^{-1}$ ).<sup>53</sup> By solid-state  $^{13}C$  MAS NMR spectroscopy, we found that decomposition of surface methoxy species at 523 K and above is responsible for the formation of first hydrocarbons on zeolites H–Y and H–ZSM-5 and on silicoaluminophosphate H–SAPO-34.<sup>17c,d</sup> A very recent investigation<sup>61</sup> on the conversion of chloromethane on H–SAPO-34 indicated that chloromethane can be efficiently converted to light olefins in the temperature range 623 to 773 K. The in situ IR observations clarified the formation of surface methoxy species as intermediate products.<sup>61</sup> Decomposition of surface methoxy species and coke deposition from incomplete calcinations are suggested as possible origins for the formation of the first reaction centers.<sup>61</sup>

Concerning the detailed mechanism for the C–H bond activation upon decomposition of surface methoxy species, it has been suggested<sup>42b,46</sup> that reactive intermediates with a carbene or ylide nature are very likely formed. Indirect evidence for the existence of carbene as a transient species was, for example, obtained by using cyclohexane as a trapping agent during the decomposition of surface methoxy species.<sup>17c</sup> The formation of methylcyclohexane implies the transient existence

of carbene which undergoes the typical  $sp^3$  insertion into the C–H bonds.<sup>17c</sup> The oxidation reaction of surface methoxy species in this contribution might be looked upon as additional evidence for the carbene mechanism. According to Hutchings and Hunter,<sup>42b</sup> the formation of formic acid upon the oxidation of surface methoxy species indicates the existence of carbene which further reacts with oxygen via the Criegee intermediate.<sup>62</sup> Furthermore, Sinclair and Catlow<sup>63</sup> performed DFT calculations to investigate the decomposition of surface methoxy species on acidic zeolites and showed that surface-stabilized carbene (**1A** in Figure 7) could be produced with an activation barrier of  $215$ – $232\text{ kJ mol}^{-1}$ . The deprotonation step (from **1C** to **1A** in Figure 7) was, therefore, suggested as the rate-determining step during the conversion of methanol to hydrocarbons. In agreement with the value reported by Sinclair and Catlow,<sup>63</sup> Lesthaeghe et al.<sup>64</sup> recently calculated a theoretical barrier of  $241\text{ kJ mol}^{-1}$  for the deprotonation of surface methoxy species to carbene. Considering this step as a highly activated one, however, they ruled out the deprotonation of methoxy species to carbene as a possible direct route for the first C–C bond formation during methanol conversion.<sup>64</sup> It was recently claimed,<sup>65</sup> in contradiction to a number of previous investigations,<sup>66</sup> that the C–H bonds of surface methoxy species are not broken at temperatures between 573 and 623 K, supported by the absence of H/D exchange between  $CH_3$ –SAPO-34 and  $CD_3$ –SAPO-34 coexisting on the catalyst. However, direct evidence for the failure of C–C bond formation from these surface methoxy species, i.e., the yields of olefin products and the H/D distribution in these olefins were not disclosed therein,<sup>65</sup> although GC and GC–MS were applied to analyze the effluent gases.

## Conclusions

The in situ stopped-flow protocol we developed<sup>17</sup> opens a new approach to the understanding of the nature of surface methoxy species on solid acid catalysts. On the basis of this development, the main focus of this contribution is, therefore, to further investigate the chemical reactivity of surface methoxy species in acidic zeolites. With the application of solid-state  $^{13}C$  MAS NMR spectroscopy, the following evidence for the high reactivity of surface methoxy species are obtained for the first time on solid acid catalysts:

(i) Surface methoxy species react with ammonia on acidic zeolite H–Y and silicoaluminophosphate H–SAPO-34 at room temperature, by which methylamines and methylammonium

(62) For the detailed discussion of Criegee mechanism, through which the carbonyl oxide is formed by the combination of carbene and oxygen, for example, see: Bunnelle, W. H. *Chem. Rev.* **1991**, *91*, 335–362. One of the referees of this manuscript suggests an alternative mechanistic proposal for the oxidation of surface methoxy species, which consists of a hydride abstraction from gas-phase methanol by surface methoxy species to form methane and formaldehyde. The  $^{13}C$  MAS NMR signal of methane (at ca.  $-9\text{ ppm}$ ) was observed in Figure 6d and 6e upon thermal treatments at 573 and 673 K, respectively. Therefore, the latter possibility cannot be absolutely ruled out, although methane formation is hardly observed at 493 and 523 K (see Figure 6b and 6c).

(63) Sinclair, P. E.; Catlow, C. R. A. *J. Phys. Chem. B* **1997**, *101*, 295–298.

(64) Lesthaeghe, D.; Van Speybroeck, V.; Marin, G. B.; Waroquier, M. *Angew. Chem., Int. Ed.* **2006**, *45*, 1714–1719.

(65) Marcus, D. M.; McLachlan, K. A.; Wildman, M. A.; Ehresmann, J. O.; Kletnieks, P. W.; Haw, J. F. *Angew. Chem., Int. Ed.* **2006**, *45*, 3133–3136.

(66) For experimental evidence of the C–H bond activation upon decomposition of surface methoxy species, for example, see the references listed in Table 1. Some of additional evidence was presented in: (a) Novakova, J.; Kubelkova, L.; Dolejs, Z. *J. Catal.* **1986**, *97*, 277–279. (b) Perot, G.; Cormerais, F. X.; Guisnet, M. *J. Mol. Catal.* **1982**, *17*, 255–260. (c) Perot, G.; Cormerais, F. X.; Guisnet, M. *J. Chem. Res. Synop.* **1982**, *2*, 58–59.

(61) Wei, Y.; Zhang, D.; Liu, Z.; Su, B. *J. Catal.* **2006**, *238*, 46–57.

cations are formed. On the contrary, methanol and ammonia do not react on acidic zeolites at room temperature. The significant difference in reactivity between surface methoxy species and methanol indicates that surface methoxy species are very reactive in methylating amines on acidic zeolites and, if involved, their formation is the rate-determining step during the methylation of amines by methanol on acidic zeolites.

(ii) The transformation of surface methoxy species to surface ethoxy species or other alkoxy species can be achieved by the reaction of surface methoxy species and corresponding alkyl halides on acidic zeolites. This new approach may provide a general method for the preparation of surface alkoxy species from surface methoxy species on solid acid catalysts.

(iii) Surface methoxy species react readily with hydrochloride, by which methyl chloride is produced as the sole product. These results indicate that surface methoxy species may be involved in methanol hydrochlorination on solid catalysts, which agrees well with the recent investigations of methanol hydrochlorination on an  $\eta$ -alumina catalyst by means of TPRS.<sup>30</sup>

(iv) The classic Koch carbonylation reaction and Ritter reaction in solution can be realized with surface methoxy species on acidic zeolites. In agreement with the recent work of Iglesia and co-workers,<sup>38</sup> the carbonylation of dimethyl ether by carbon

monoxide on acidic zeolites is interpreted as similar to the classic Koch-type reaction in solution, where the unstable acylium cation,  $\text{CH}_3\text{—C}^+=\text{O}$ , is formed by the reaction of surface methoxy species and CO. In accordance with the Ritter-type reaction on solid acid catalysts,<sup>39</sup> the formation of *N*-methyl acetamide was interpreted by further hydrolysis of the intermediate, the *N*-alkylnitrilium cation, after the reaction of surface methoxy species and acetonitrile on acidic zeolites.

(v) Carbon monoxide and carbon dioxide can be produced by the oxidation of surface methoxy species on acid zeolites in the presence of oxygen. The oxidation of surface methoxy species may compete with the thermal decomposition of surface methoxy species. However, oxygen may not play an active role to initiate the formation of primary hydrocarbons in the induction period of the MTO process.

**Acknowledgment.** The Deutsche Forschungsgemeinschaft, the Max-Buchner-Forschungsstiftung, and the Fonds der Chemischen Industrie provided financial support, which the authors gratefully acknowledge. W.W. thanks the Chunhui Project of Education Ministry of P. R. China. We are grateful to the anonymous reviewers for their valuable comments and suggestions.

JA061018Y